

14(R,S)-[¹⁸F]Fluoro-6-Thia-Heptadecanoic Acid (FTHA): Evaluation in Mouse of a New Probe of Myocardial Utilization of Long Chain Fatty Acids

Timothy R. DeGrado, Heinz H. Coenen, and Gerhard Stöcklin

Institut für Chemie 1, Forschungszentrum Jülich, Germany

14(R,S)-[¹⁸F]Fluoro-6-thia-heptadecanoic acid (FTHA) is a new radiolabeled long-chain fatty acid (LCFA) analog designed to undergo metabolic trapping subsequent to its commitment to the β -oxidation pathway. Sulfur-substitution at the sixth carbon of FTHA causes a prolonging of myocardial clearance half-time ($T_{1/2} \sim 2$ hr) in mice with little diminution of myocardial uptake ($39.8 \pm 3.0\%$ ID/g at 5 min). Heart-to-blood ratios were 20 ± 6 and 82 ± 16 at 1 and 60 min, respectively. In contrast, the 3-thia analog, 13(R,S)-[¹⁸F]-fluoro-3-thia-hexadecanoic acid, showed lower uptake and poor retention by heart. Myocardial uptake of FTHA was reduced by 81% ($p < 10^{-5}$) and 87% ($p < 5 \times 10^{-4}$) in mice pretreated with the carnitine palmitoyltransferase I inhibitor, 2[5(4-chlorophenyl)pentyl]oxirane-2-carboxylate (POCA) at 1 and 60 min, respectively. Radioanalytical studies showed the major metabolic fate of FTHA in control and POCA treated myocardium to be unidentified metabolite(s) that bind to tissue protein. Smaller amounts of ¹⁸F radioactivity were present in myocardium as complex lipids, fatty acid, and unidentified soluble metabolites. The results indicate metabolic trapping of FTHA in myocardium subsequent to its entry into the mitochondrion and encourage its further evaluation as a PET tracer of myocardial LCFA utilization.

J Nucl Med 1991; 32:1888-1896

The noninvasive assessment of regional myocardial oxidative metabolism by PET has been recently forwarded with the use of [¹¹C]acetate (1,2). A variety of exogenous substrates can be utilized by heart for provision of acetyl-CoA to the tricarboxylic acid cycle. These include fatty acids, glucose, and lactate. Although β -oxidation of long-chain fatty acids (LCFAs) represents the major source of mitochondrial acetyl-CoA in normal conditions, the profile of substrate utilization is sensitive to nutritional, metabolic, and pathologic alterations (3-4). A PET technique for measurement of regional LCFA β -oxidation rate would

therefore provide important information toward the characterization of oxidative substrate metabolism in the myocardium.

[1-¹¹C]palmitate (CPA) has been investigated as a natural tracer of fatty acid metabolism (4-7). Both release of the oxidative catabolite, ¹¹CO₂, and backdiffusion of CPA contribute to the early myocardial clearance pattern. Since the diffusion rates of ¹¹CO₂ and unoxidized CPA are both rapid, the fractional contribution of the two clearance processes cannot be determined from kinetic analysis of regional time-activity curves. As a result of this ambiguity, the interpretation of CPA kinetics in heart has remained strictly qualitative and subject to uncertainty (4-7). ω -[¹⁸F]-Fluoro LCFA analogs have myocardial uptake and clearance rates similar to radiolabeled palmitate (8-10). Six- and 7-[¹⁸F]fluoropalmitate (11) also showed uptake and clearance from heart similar to palmitate but fluorine substitution at the α -carbon of stearic acid caused a large decrease in myocardial uptake (8). The longer half-life of ¹⁸F in comparison to ¹¹C ($T_{1/2} = 110$ min versus 20 min) would allow longer PET measurement periods and off-site production of radiotracer. Otherwise, the straight chain [¹⁸F]fluoro fatty acids appear to offer no further advantage over CPA.

The β -methyl substituted analog of CPA, β -methyl-[1-¹¹C]heptadecanoic acid (BMHDA), has been proposed to provide a longer myocardial retention of the radiolabel as a consequence of inhibited β -oxidation (12-14). The primary metabolic fate of BMHDA in heart is incorporated into triglycerides and phospholipids. Preliminary studies with 3-methyl and 5-methyl substituted ω -[¹⁸F]-fluoro palmitate analogs in rats showed longer myocardial retention than ω -[¹⁸F]fluoro-palmitate (15). However, the maximal myocardial uptakes of the branched-chain ¹⁸F-labeled LCFA analogs were lower than for the straight chain analog, suggesting a steric hinderance effect on initial steps of transport and/or metabolism. Also, high uptake of radioactivity in bone indicated defluorination of both methyl-substituted LCFA analogs. β -Oxidative catabolism of LCFA analogs has also been inhibited by the use of heteroatom substitution; single-photon emitter labeled fatty acid analogs containing tellurium at positions 5-9

Received Feb. 29, 1991; revision accepted May 9, 1991
For reprints contact: Dr. G. Stöcklin, Institut für Chemie 1, Forschungszentrum Jülich, Postfach 1913, D-5170 Jülich, FRG.

TABLE 1
Biochemical Acceptance of Thia Fatty Acid Analogs and Derivatives

Chain length*	Position of sulfur atom	Enzyme/Process	Reference
15	3	acyl-CoA synthetase	20
15	3	carnitine-palmitoyl transferases	20
15	3	acyl-transferase	20
8	4	medium chain acyl-CoA dehydrogenase	18
15	3	cytochrome P-450/ ω -oxidation	21
14	6, 12	myristoyl-CoA:protein N-myristoyltransferase	23
18	10	stearyl-CoA desaturase	24

* Including sulfur atom.

show adequate myocardial uptake and long retention (16,17).

Thia fatty acid analogs have recently received interest as false substrates and/or inhibitors of fatty acid metabolism (18–24). They are accepted for many processes of LCFA metabolism (Table 1) but complete β -oxidation of the chain is blocked by the sulfur heteroatom (20–22). The thioether decreases the hydrophobicity of the chain significantly but causes only minor effects on bond length and bond angle (23). Interestingly, the CoA thioesters of 4-thia fatty acid analogs are potent inhibitors of β -oxidation (22). Acyl-CoA dehydrogenases (ACD) could possibly be inhibited by their products, 4-thia-2-enoyl-CoA thioesters (18,19).

The biochemical data, albeit limited, on 4-thia fatty acid analogs have potential application to the design of cardiac PET tracers of LCFA utilization. A terminally-labeled, even-substituted (n-thia; n = 4, 6, 8...) LCFA analog could be β -oxidized to oxidative metabolites that could possibly be retained in the myocardium. Accordingly, two ^{18}F -labeled, 6-thia LCFA analogs were proposed, synthesized, and preliminarily evaluated (25): 16- ^{18}F fluoro-6-thia-hexadecanoic acid and 14(R,S)- ^{18}F fluoro-6-thia-heptadecanoic acid (FTHA, Fig. 1).

In this paper, the in vivo distribution and metabolism of FTHA are characterized in mice. Analytical studies are aimed at defining the major metabolic fates of the radiolabel in heart and liver. The hypothesis of (oxidative) metabolic trapping is tested by observing changes in the utilization of FTHA caused by the carnitine palmitoyl-

transferase I inhibitor, 2[5(4-chlorophenyl)-pentyl]oxirane-2-carboxylate (POCA). Finally, the effect of thioether position is examined by comparative studies with the 3-thia analog, 13(R,S)- ^{18}F fluoro-3-thia-hexadecanoic acid (13F3THA, Fig. 1).

MATERIALS AND METHODS

Synthesis of Radiotracers

The no-carrier-added synthesis of FTHA was performed using an aminopolyether supported radiofluorination procedure (26) as modified from Coenen et al. (27). The chemical precursor to FTHA was benzyl 14(R,S)-tosyloxy-6-thia-heptadecanoate. 13F3THA was similarly prepared (28). The LCFA analogs were purified by reversed-phase HPLC and formulated in a saline solution containing 6% albumin (26).

Kinetics of ^{18}F -labeled LCFA Analogs in Mice

Kinetics of ^{18}F radioactivity were measured in male NMRI mice (25–30 g) in heart, blood, liver, kidney, lung, and bone (taken from cranium) after tail-vein injections of radiotracer (1–10 μCi). Mice were fed *ad libidum*. Groups of 3–4 mice were euthanized at times of 0.25–120 min postinjection. For FTHA, two groups were studied: control and POCA treated. The later group received intraperitoneal administration of POCA (sodium salt, 40 mg/kg, generously provided by Dr. H.P.O. Wolf, Byk-Gulden Lomberg Chemische Fabrik, Konstanz, FRG) 2–3 hr prior to injection of radiotracer.

Analysis of ^{18}F Radioactivity in Tissues

Analytical studies were performed to determine the chemical nature of the ^{18}F radioactivity retained in blood, heart, and liver. The organs were excised from mice at prescribed times after injections of radiotracer (15–50 μCi). A portion of tissue (~0.15 g) was rinsed in chilled saline, blotted to remove excess liquid, placed into 1.25 ml chloroform/methanol (2:1) at 0°C and rapidly homogenized (2 \times 15 sec bursts at high speed) with a Polytron. Following ultrasonication for 15 sec, 0.35 ml aqueous urea (40%) and 0.35 ml 5% sulfuric acid were added. The mixture was ultrasonicated (15 sec) and centrifuged at 2,500 g for 5 min. The total ^{18}F radioactivity in each tube was measured. The aqueous, organic, and pellet fractions were separated and counted.

The organic fraction was extracted again with 5% sulfuric acid and subjected to thin-layer chromatography (TLC) analysis on aluminum-backed silica gel layers developed with petroleum

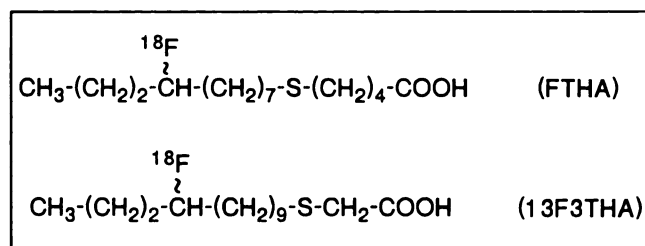


FIGURE 1. Molecular structures of ^{18}F -labeled, thia LCFA analogs.

ether/ether/acetic acid (70:30:1). The lipid bands were visualized by exposing the layers to iodine vapors and identified with reference to R_f values of lipid standards. The layers were cut into strips corresponding to the identified lipid bands and counted. The approximate R_f values used were: phospholipids (PL, 0.0–0.1), diglycerides (DG, 0.2–0.3), fatty acids (FA, 0.4–0.5), triglycerides (TG, 0.8–0.9), and cholesterol esters (CE, 0.9–1.0).

The binding of ^{18}F radioactivity to pellet fractions was further investigated in three groups of hearts taken from control mice euthanized 5 min after injection of FTTHA. After extraction of the whole heart homogenate as described above, the pellet fraction was dissolved in 1N NaOH (1 ml) at 90°C for 1 hr. For the first group (n = 3), the protein was directly precipitated by the addition of 1 ml 50% trichloroacetic acid (TCA). After centrifugation, the aqueous and pellet phases were separated and counted. For the remaining two groups, the alkalinity of the mixture was first adjusted to pH = 8.4 by addition of sodium bicarbonate and glacial acetic acid. For the second group (n = 3), 2 ml chloroform/methanol (2:1) was added and the mixture was ultrasonicated. After the addition of 1 ml 50% TCA, the sample was centrifuged, and the organic, aqueous, and pellet phases were separated and counted. The third group (n = 3) was incubated with 75 mg dithiothreitol (29) for 5 min at pH = 8.4. Further treatment with chloroform/methanol and 50% TCA was identical to that of the second group.

Determination of [^{18}F]fluoride in Biologic Samples

To a 20-ml scintillation counting vial was added 0.1–1.0 ml of sample. A small polypropylene bucket containing 0.8 ml 1N NaOH was secured through a silicone rubber stopper and suspended 2 cm below the stopper. Immediately after the addition of 0.1 ml chlorotrimethylsilane to the bottom of the vial, the vial was sealed. After incubation for 1 hr at 50°C, the bucket and vial were counted separately. Gaseous [^{18}F]fluorotrimethylsilane (^{18}F -TMS) produced from [^{18}F]fluoride in the sample was carried to the bucket where the [^{18}F]fluoride was regenerated upon hydrolysis (30). Values were expressed as the percentage of radioactivity recovered in the bucket. Control samples containing [^{18}F]fluoride showed 97% ± 2% recovery. Standards of FTTHA and 13F3THA showed <0.05% recovery.

Statistical Analysis

Data are expressed as means ± standard error. The t-test (two-tailed) for unpaired samples was used to compare means from control and POCA-treated mice.

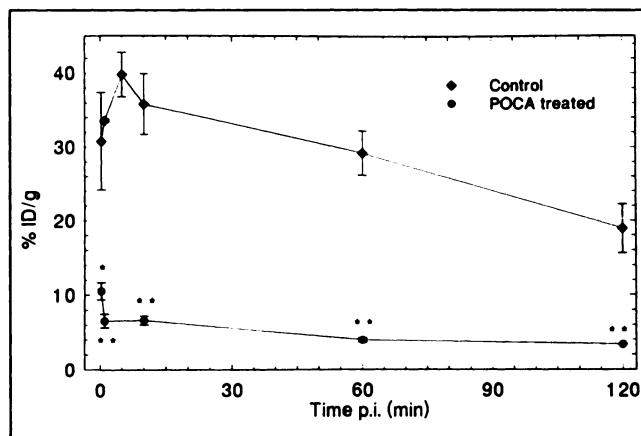


FIGURE 2. Effects of POCA on myocardial kinetics of ^{18}F radioactivity in mouse following intravenous administration of FTTHA. Significance versus control: * ($p < 0.001$), ** ($p < 10^{-5}$)

RESULTS

FTTHA Kinetics in Normal Mice

Following intravenous injection of FTTHA in untreated mice, the concentration of ^{18}F radioactivity in the blood declines rapidly, showing rapid transport of the tracer to the tissues (Table 2). Uptake of ^{18}F radioactivity was highest in heart, reaching $39.8 \pm 3.0\%$ ID/g at 5 min. The subsequent clearance of radioactivity from heart was slow, showing a half-clearance time of about 2 hr (Fig. 2). Heart: blood ratios of uptake were 4.3 ± 0.4 , 20 ± 6 , 41 ± 6 , and 82 ± 16 at 0.25, 1, 5 and 60 min, respectively. The liver also showed high uptake of radioactivity, reaching a maximum of $23.4 \pm 3.5\%$ ID/g at 5 min. Hepatic clearance of radioactivity in the first hour was faster than that of heart ($T_{1/2} \sim 30$ min). Heart: liver ratios decreased from 3.2 ± 0.5 at 15 sec to 1.6 ± 0.2 at 1 min, but increased thereafter. Lung uptake was low relative to that of heart, showing heart: lung ratios of 4.7–13.6. The kidneys showed uptake of radioactivity at early times ($20.5 \pm 3.7\%$ ID/g at 5 min) and significant clearance over the first hour. ^{18}F radioactivity slowly accumulated in bone over the first hour to a level of $\sim 4\%$ ID/g.

TABLE 2
Distribution of ^{18}F Radioactivity in Control Mice After Intravenous Injection of FTTHA (% ID/g, n = 3–4 at Each Interval)

Time (min)	Heart	Blood	Liver	Lung	Kidney	Bone
0.25	30.8 ± 5.7	7.3 ± 1.7	10.0 ± 3.4	6.6 ± 0.8	15.6 ± 6.2	1.8 ± 0.1
1	33.6 ± 0.2	1.8 ± 0.5	21.7 ± 3.5	6.1 ± 0.3	18.6 ± 2.7	2.3 ± 0.5
5	39.8 ± 3.0	1.00 ± 0.16	23.4 ± 3.5	6.9 ± 0.6	20.5 ± 3.7	2.3 ± 0.2
10	35.8 ± 4.1	1.15 ± 0.23	21.7 ± 1.8	5.3 ± 0.7	18.1 ± 0.8	2.1 ± 0.5
60	29.2 ± 3.0	0.36 ± 0.04	8.9 ± 1.5	2.3 ± 0.6	6.1 ± 1.2	4.3 ± 0.5
120	18.9 ± 3.3	0.28 ± 0.05	5.5 ± 0.7	2.0 ± 0.4	4.9 ± 0.4	3.8 ± 1.3

TABLE 3
Distribution of ¹⁸F in Tissues after Intravenous Injection of FTTHA (% Total Radioactivity, n = 3 Each)

Organ, Group	Time (min)	Organic	Aqueous	Pellet	Recovery	[¹⁸ F]F ⁻
Blood, C	10	36.3 ± 2.4	38.7 ± 1.4	20.3 ± 2.9	95 ± 2	25.0 ± 0.5
P	10	41.1 ± 3.6	34.3 ± 1.9	20.1 ± 1.3	96 ± 2	17.5 ± 2.8 [†]
Heart, C	1	12.9 ± 1.5	2.3 ± 0.3	84.4 ± 3.5	99 ± 1	n.a.
	10	6.1 ± 0.8	2.0 ± 0.0	84.9 ± 1.7	93 ± 2	0.6 ± 0.1
	60	5.8 ± 1.3	5.5 ± 1.5	82.6 ± 10.9	94 ± 8	n.a.
P	1	49.1 ± 6.6 [§]	1.4 ± 0.8	48.8 ± 6.6 [§]	99 ± 1	n.a.
	10	37.6 ± 1.3 [†]	10.4 ± 1.3 [§]	45.4 ± 2.4 [†]	93 ± 4	6.5 ± 0.2 [†]
	60	26.1 ± 1.4 [†]	12.3 ± 1.7 [‡]	63.6 ± 2.7 [†]	97 ± 3	n.a.
Liver, C	10	21.8 ± 2.2	18.3 ± 0.9	57.5 ± 1.9	98 ± 1	4.6 ± 0.4
P	10	34.7 ± 2.0 [‡]	18.8 ± 4.7	42.4 ± 4.3 [†]	96 ± 9	5.8 ± 1.2

Significance versus control: [†] p < 0.05; [‡] p < 0.01; [§] p < 0.001; [¶] p < 0.0001.
C = control and P = POCA treated.

Analysis of ¹⁸F Radioactivity in Tissues

To define the metabolic pathways available to FTTHA in heart and peripheral tissues, the chemical form of the ¹⁸F radioactivity in blood, heart, and liver was investigated (Tables 3 and 4). First, tissues were homogenized in chloroform/methanol (2:1) and extracted with 20% urea in 2.5% sulfuric acid. After centrifugation, the organic, aqueous, and pellet phases were separated and counted (Table 3). At least five radioactivity peaks were present in the organic phase (Table 4). Four of these were designated from their R_f values as radiolabeled phospholipids (PL), diglycerides (DG), fatty acids (FA), and triglycerides (TG). No designation was made for the radioactivity peak at R_f = 0.3–0.4.

The blood showed both organic and aqueous soluble components of ¹⁸F radioactivity. [¹⁸F]fluoride accounted for 66% of the aqueous soluble radioactivity or ~0.3% ID/g at 10 min (Table 3).

FTTHA was rapidly metabolized in hearts of control animals. At 1 min p.i., less than 2% of the radioactivity in heart could be accounted for as FA (Tables 3 and 4). The pellet phase contained the largest fraction of radioactivity

(~85%) at all measured intervals. The ¹⁸F-labeled, acid soluble fraction rose from 2% at 1 min to 6% at 60 min. At 10 min, 30% of the acid soluble ¹⁸F radioactivity was identified as [¹⁸F]fluoride, representing a content of ~0.2% ID/g (Table 3). The organic soluble fraction was 13% at 1 min and decreased with time. TLC analysis of the organic phase (Table 4) showed more ¹⁸F radioactivity in PL (62%–68%) than in TG (8–14%) or in DG (4–10%).

Efforts to release the radioactivity bound to the protein by dissolution in hot aqueous NaOH and reprecipitation with trichloroacetic acid (TCA) were partially successful. Pellets were analyzed in three groups. In the first group, less than 2% of the ¹⁸F radioactivity was not bound to protein after direct precipitation with TCA. In the second group, the alkalinity of the dissolved protein solution was first adjusted to pH = 8.4 and chloroform/methanol was added and mixed. Protein was then precipitated by the addition of TCA. This group showed 30% ± 3% of the ¹⁸F radioactivity released to the organic phase, 2.2% ± 1.0% released to the aqueous phase, and 68% ± 4% remaining with the protein. The third group was treated with dithiothreitol before extraction with chloroform/methanol. This

TABLE 4
Silica Gel TLC Analysis of Organic Soluble Metabolites of FTTHA (% Organic Soluble ¹⁸F Radioactivity, n = 3–4 at Each Interval in Mice Hearts and Livers)

Tissue, group	Time p.i. (min)	Fraction (R _f range)				
		PL (0.0–0.1)	DG (0.2–0.3)	unknown (0.30–0.40)	FA (0.4–0.5)	TG (0.8–0.9)
Heart, C	1	61.7 ± 6.3	3.5 ± 1.3	9.8 ± 7.2	9.6 ± 1.3	14.3 ± 4.7
	10	68.5 ± 10.7	10.2 ± 4.6	3.8 ± 0.5	7.4 ± 3.9	7.9 ± 4.8
Heart, P	1	17.1 ± 1.0 [§]	6.9 ± 2.0	47.5 ± 1.5 [‡]	25.2 ± 2.3 [†]	2.3 ± 0.5 [†]
	60	32.8 ± 14.1	12.4 ± 6.8	13.1 ± 10.3	2.3 ± 0.7	36.9 ± 17.8
Liver, C	10	67.2 ± 3.0	3.7 ± 1.0	1.4 ± 0.1	21.4 ± 2.4	4.9 ± 0.9
Liver, P	10	50.7 ± 2.5 [‡]	3.1 ± 1.1	1.9 ± 0.5	37.2 ± 2.1 [†]	5.0 ± 1.0

Significance versus control: [†] p < 0.05; [‡] p < 0.01; [§] p < 0.001; [¶] p < 0.0001.
C = control, P = POCA treated, PL = phospholipids, DG = diglycerides, FA = fatty acids, TG = triglycerides.

was intended to free from protein any metabolites conjugated through disulfide bonds (29). This group showed $34\% \pm 4\%$ and $0.6\% \pm 0.2\%$ of ^{18}F radioactivity in the organic and aqueous phases, respectively.

At 10 min, the liver showed the highest fraction of ^{18}F radioactivity as hydrophilic metabolites (18%, Table 3). About 25% of this radioactivity was [^{18}F]fluoride, representing a content of $\sim 1.0\%$ ID/g (Tables 2 and 3). Thus, at 10 min, the concentration of [^{18}F]fluoride was about three times higher in the liver than in blood. Higher levels of ^{18}F -labeled organic soluble species, including FA, were found in liver than in heart (Tables 3 and 4).

Effects of POCA on the Biodistribution and Metabolism of FTHA

The myocardial accumulation of ^{18}F radioactivity in mice was dramatically reduced by pretreatment with the carnitine palmitoyl-transferase I inhibitor, POCA (Table 5, Fig. 2). The highest measured heart uptake was $10.5 \pm 1.2\%$ ID/g at 15 sec. At early times, the concentration of radioactivity in heart followed closely that in blood; heart:blood ratios were near unity within the first minute but increased gradually to 13 ± 2 at 2 hr. POCA caused decreases in ^{18}F radioactivity uptake by heart of 81%, ($p < 10^{-5}$) and 87% ($p < 5 \times 10^{-4}$) at 1 and 60 min, respectively. Liver uptake of FTHA in POCA-treated mice was significantly higher than that of controls at 5 min ($p < 0.01$) and 10 min ($p < 0.05$), but was not different at the other measurement intervals. The uptakes in kidney and lung were not significantly affected by treatment with POCA. Accumulation of radioactivity in bone was higher in the POCA-treated group, reaching $9.2 \pm 0.6\%$ ID/g at 2 hr ($p < 0.01$).

POCA caused reductions of the pellet fraction in heart and liver. When expressed in the same units of uptake (%ID/g), POCA caused a 90% reduction ($p < 10^{-4}$) of pellet-bound ^{18}F radioactivity in heart at 1 hr (Tables 2, 3, and 5). For liver, however, the content of ^{18}F -labeled, pellet-bound products was not significantly altered by POCA.

Changes with POCA were observed in the production of lipophilic metabolites. Although the myocardial uptake of ^{18}F radioactivity was dramatically reduced by POCA,

the content of ^{18}F -labeled FA (presumably FTHA) within the myocardium was increased (Tables 2–5). For example, ^{18}F -labeled FA content in POCA treated heart at 1 min ($\sim 0.8\%$ ID/g) was approximately twice that of control. The total organic fraction of ^{18}F radioactivity was also higher, representing 49% and 26% of the total ^{18}F radioactivity in heart at 1 and 60 min, respectively (Table 3). The TG:PL ratio was higher in POCA treated hearts relative to controls and increased with time (Table 4). The unidentified lipophilic metabolite showing an R_f of 0.3–0.4 with silica gel TLC was more prevalent in POCA-treated heart. This entity was either cleared from myocardium or metabolized over time (Table 3). In liver, POCA significantly increased the organic soluble fraction of ^{18}F radioactivity at 10 min (Table 3). The fraction of the organic phase as FA was increased with POCA (Table 4). The fraction as PL was correspondingly decreased. The TG:PL ratio was only slightly increased in liver treated with POCA.

The formation of hydrophilic metabolites from FTHA was also enhanced by POCA. The content of [^{18}F]fluoride in the blood of POCA treated mice at 10 min was approximately 0.36% ID/g (Tables 3 and 5). This was 25% higher ($p < 0.05$) than that of controls. The heart and liver showed 100% ($p < 10^{-4}$) and 82% ($p < 0.005$) increases of [^{18}F]fluoride content with POCA, respectively. POCA caused an increase of 48% ($p < 0.05$) in the content of all aqueous soluble metabolites in liver at 10 min (Tables 2, 3, and 5). In contrast, POCA did not effect a significant increase in heart content of hydrophilic metabolites, although their fractional contribution to the total ^{18}F radioactivity in heart was higher at later times (Table 3).

Effect of Thia Position

Comparative studies with even-substituted FTHA and odd-substituted 13F3THA were performed to show the influence of the thia position on the in vivo kinetics of ^{18}F -labeled thia LCFA analogs. Uptake of ^{18}F radioactivity by mouse heart was higher with FTHA than with 13F3THA (Fig. 3). Myocardial clearance was faster for the 3-thia analog. Liver uptake of 13F3THA was higher than that of FTHA (Fig. 3). Hepatic clearance, especially in the second hour after injection, was also faster with 13F3THA than with FTHA.

TABLE 5
Distribution of ^{18}F Radioactivity in POCA-Treated Mice Following Intravenous Injection of FTHA (%ID/g, $n = 3-4$ at Each Interval)

Time (min)	Heart	Blood	Liver	Lung	Kidney	Bone
0.25	10.5 ± 1.2	9.7 ± 2.5	10.9 ± 2.7	8.4 ± 1.2	15.3 ± 6.2	2.2 ± 0.6
1	6.5 ± 0.9	4.5 ± 0.5	25.2 ± 1.9	6.3 ± 0.7	21.3 ± 1.9	4.3 ± 1.1
5	6.2 ± 0.5	2.42 ± 0.25	36.1 ± 1.9	7.1 ± 1.2	23.0 ± 2.2	5.9 ± 1.6
10	6.6 ± 0.6	2.08 ± 0.11	31.3 ± 4.1	6.6 ± 0.6	19.1 ± 0.7	4.5 ± 0.2
60	3.9 ± 0.3	0.44 ± 0.02	9.7 ± 0.8	1.8 ± 0.2	5.7 ± 0.4	6.3 ± 0.5
120	3.3 ± 0.1	0.27 ± 0.04	6.4 ± 1.4	1.8 ± 0.1	3.9 ± 0.6	9.2 ± 0.6

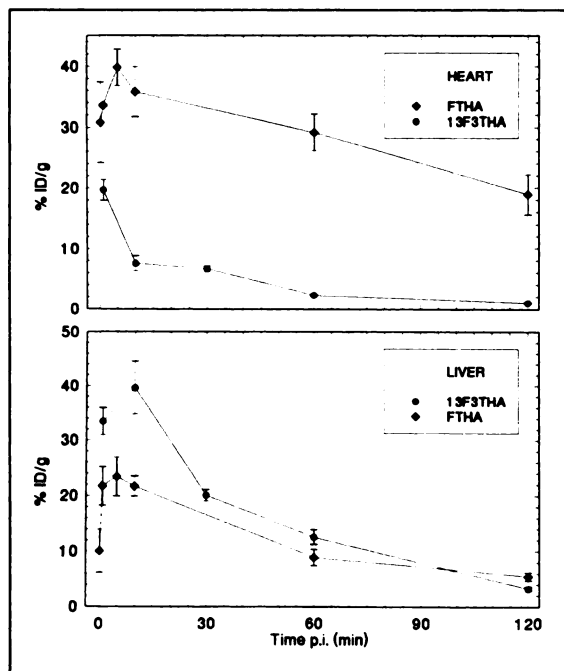


FIGURE 3. Effects of position of the sulfur atom on myocardial and hepatic kinetics of ^{18}F radioactivity following intravenous injection of ^{18}F -labeled thia LCFA analogs in mouse.

DISCUSSION

The ability of the new ^{18}F -labeled LCFA analog, FTHA, to be transported into myocardium and undergo initial steps of metabolism is shown from its high uptake by mice hearts ($\sim 40\%$ ID/g at 5 min) and the early formation of metabolic products within the tissue (Tables 3 and 4). The maximal myocardial uptakes in mice of $[1\text{-}^{11}\text{C}]$ palmitate ($43 \pm 8\%$ ID/g at 0.5 min) and $17\text{-}[^{18}\text{F}]$ fluoroheptadecanoic acid ($41 \pm 11\%$ ID/g at 0.25 min) are equivalent (8,31). This would suggest that neither the sulfur heteroatom at the sixth position nor the fluorine at carbon-14 of FTHA significantly hinders the multi-step translocation of FTHA from binding sites of albumin within the plasma to binding sites of fatty acid binding protein (FABP) within the myocyte (32). Activation of FTHA to its acyl-CoA (FTHA-CoA) is also implied because it is this step which sequesters fatty acids within myocardium and precedes further metabolism (3).

Comparative studies with mice pretreated with the CPT I inhibitor, POCA, strongly imply that the rapid accumulation in heart of protein-bound ^{18}F radioactivity with injection of FTHA is a consequence of some metabolic process associated with β -oxidation. POCA caused an 80%–90% decrease in myocardial ^{18}F radioactivity after intravenous injection of FTHA in mice (Fig. 2). This dramatic effect was seen as early as 1 min after injection. When the 30%–40% lower pellet-bound fractions of ^{18}F radioactivity in POCA treated heart are considered, the association between the capacity of the heart to β -oxidize LCFA and the formation of protein-bound metabolite(s)

becomes even stronger. In normal rat myocardium, similar treatment with POCA causes a reduction of $\sim 90\%$ in the oxidation rate of palmitate (33,34). Thus, the decrease in ^{18}F radioactivity content with POCA after 1 min accords with the expected inhibition of LCFA β -oxidation rate. In this respect, our results corroborate those of Wyns et al. (7) showing the effects of another inhibitor of CPT I, 2-tetradecylglycidic acid (TDGA), on CPA kinetics in canine myocardium. They observed a 34% diminution of CPA single-pass retention fraction with TDGA, which compared with the 41% decrease in measured myocardial fatty acid consumption. Otherwise, the myocardial time-activity curves were similar.

The effect of POCA on myocardial blood flow was not measured, though previous studies have shown it to be negligible in normal rodent myocardium (33–35). The data would therefore suggest that myocardial blood flow determines the delivery of FTHA to the myocardium but retention of ^{18}F radioactivity is dependent on subsequent steps of metabolism. The possibility that long chain acyl-CoA synthetase (LCACS) was directly inhibited by POCA with the dosage used in our studies is unlikely. High levels of cytosolic long chain acyl-CoA and long chain acyl-carnitines resulting from inhibition of CPT I by POCA could inhibit LCACS (3). A decrease of LCFA activation concordant with the inhibition of β -oxidation would explain the low heart: blood ratios with POCA even at early times.

Comparative studies with the 3-thia LCFA analog, 13F3THA, showed several effects of the position of the sulfur atom (Fig. 3). 13F3THA showed lower myocardial uptake and faster clearance rates of ^{18}F radioactivity from the myocardium. β -Oxidation of 3-thia fatty acids is entirely blocked (20–22). They are, however, substrates of CPT, acyl transferase, and ω -hydroxylase (20–21). Analysis of ^{18}F radioactivity in hearts administered 13F3THA did not show a significant fraction in the pellet phase (data not shown). Thus, the myocardial accumulation and retention of protein-bound ^{18}F radioactivity was specific to only the even-substituted thia LCFA analog. The sulfur atom at the third position of 13F3THA may retard initial steps of transport and/or metabolism due to its proximity to the carboxyl group. Therefore, the genuine “odd-even effect” would be better indicated by comparison of FTHA with a similar LCFA analog substituted at carbon 5 or 7.

The metabolic handling of FTHA along the β -oxidation pathway and the subsequent formation of protein-bound metabolites have not been elucidated. FTHA is presumably β -oxidized to $12\text{-}[^{18}\text{F}]$ fluoro-4-thia-2-pentadecanoyl-CoA and $12\text{-}[^{18}\text{F}]$ fluoro-4-thia-3-hydroxy-pentadecanoyl-CoA within the mitochondrion. The biologic lifetime of the former may be lengthened through reversible binding to long chain acyl-CoA dehydrogenase (*cf.* 19). Failure to release $\sim 70\%$ of the ^{18}F radioactivity from pellet fractions (derived from normal myocardium at 5 min p.i.) after dissolution in hot aqueous NaOH strongly implies cova-

lent bonding of this fraction of ^{18}F radioactivity to protein. The lack of effect of dithiothreitol on the release of radioactivity from protein would suggest that disulfide linkage plays a minor role if any. In vitro results of Lau et al. (18, 19) show that 4-thia-octanoyl-CoA is a good substrate of medium chain acyl-CoA dehydrogenase. The resulting 4-thia-2-octenoyl-CoA is slowly hydrated by enoyl-CoA hydratase to form 4-thia-3-hydroxy-octanoyl-CoA. The thiohemiacetal undergoes nonenzymatic fragmentation, releasing malonylsemialdehyde-CoA and butanethiol. These observations agree with the recent finding that metabolism of $[1-^{14}\text{C}]$ -4-thia-octadecanoic acid in isolated liver mitochondria results in the formation of labeled malonate semialdehyde (Drs. E. Hrattum, J. Bremer, Institute of Medical Biochemistry, University of Oslo personal communication). Given this fragmentation, one explanation of the inhibition of β -oxidation by 4-thia fatty acid analogs (22) would be inactivation of an enzyme critical to β -oxidation by conjugation with the sulfur-containing fragment. This mechanism-based inhibition could be evidenced by the incorporation of radioactivity into protein upon β -oxidation of an even-substituted thia fatty acid analog, radiolabeled at a terminal position. Indeed, the finding of protein-bound metabolites of FTTHA is consistent with such a mechanism. Alternatively, the malonylsemialdehyde-CoA fragment, or a subsequent metabolite, could be responsible for the inhibition of β -oxidation. Malonyl-CoA reversibly inhibits CPT I (36). In this case, the binding of the sulfur-containing fragment to protein could be merely consequential. Whether the conjugation of the ^{18}F -labeled metabolite of FTTHA to protein takes place after formation of the free thiol, 8- $[^{18}\text{F}]$ fluoro-undecane-1-thiol, remains to be shown. We could find no information on the metabolic fate of long chain alkylthiols. However, binding of short chain alkyl-thiols to cytochrome c and cytochrome c oxidase has been reported (37).

It is not clear what causes the slow clearance of ^{18}F radioactivity in normal myocardium after 5 min (Fig. 2). Myocardial clearance of radioactivity as a result of turnover of complex lipids or loss of lipophilic metabolite(s) could account for only a small fraction of this clearance: the decrease in ^{18}F radioactivity content over the period 10–120 min ($\sim 17\%$ ID/g, Table 2) far exceeds the amount of ^{18}F -labeled, organic soluble species at 10 min ($\sim 2\%$ ID/g, Tables 2 and 3). Thus, a significant fraction of the protein-bound pool of ^{18}F radioactivity is released over the first 2 hr. If the same clearance occurs in human, then dynamic tomographic imaging and kinetic modeling would be required to account for this loss for accurate estimation of the tracer utilization rate.

FTTHA is apparently incorporated into complex lipids, the predominant fate being phospholipids (Table 4). Incorporation into triglycerides is relatively low. Radiolabeled palmitate shows a discrepant pattern of complex lipid incorporation in heart with triglyceride:phospholipid

fractions of ~ 5 in normal myocardium (38,39). Inhibition of β -oxidation with POCA increased the complex lipid fraction of ^{18}F radioactivity and the triglyceride:phospholipid ratio. If the protein-bound fraction of ^{18}F radioactivity is considered to be the fraction of FTTHA-CoA undergoing β -oxidation, then 80%–90% of FTTHA-CoA is oxidized and 5%–10% is esterified in normal myocardium (Table 3). Since FTTHA may have lipophilic metabolites other than those designated as natural occurring lipids, these interpretations should be regarded as preliminary.

The liver showed a slower accumulation of protein-bound metabolites of FTTHA and a higher incorporation of tracer into complex lipids than in heart. In contrast to the heart, the undiminished hepatic uptake of FTTHA with POCA may reflect the greater availability of metabolic pathways in liver which do not depend on CPT I. The hepatic uptake and retention of ^{14}C -labeled palmitate in rats (12) is comparable to these results with FTTHA. Higher concentrations of $[^{18}\text{F}]$ fluoride and other ^{18}F -labeled hydrophilic metabolites in liver than in blood indicate hepatic catabolism of FTTHA. The release of $[^{18}\text{F}]$ fluoride from liver or other organs into the bloodstream is particularly undesirable because the fluoride anion can diffuse into myocardium and accumulate in infarcted regions (40). Defluorination of non- β -oxidizable ^{18}F -labeled LCFA analogs has been recently studied (28). Bone uptake of ^{18}F radioactivity, which is a good indicator of in vivo defluorination (41), is $\sim 4\%$ ID/g at 2 hr in mice with FTTHA. This is only 25% of the bone uptake of radioactivity measured with the ω -labeled analog, 16- $[^{18}\text{F}]$ fluoro-6-thia-hexadecanoic acid (25) and about 15% of that measured with $[^{18}\text{F}]$ fluoride in mice at the same interval (41). Hepatic ω -oxidation of FTTHA could yield ω -carboxy (ω -3)- $[^{18}\text{F}]$ fluoro and ω -carboxy (ω -1)- $[^{18}\text{F}]$ fluoro catabolites of FTTHA. Further β -oxidation of the latter from the terminal end would be blocked by the presence of the $[^{18}\text{F}]$ fluorine atom (8). The sulfide moiety of thia fatty acid analogs is oxidized to sulfoxide by FAD-dependent monooxygenases in liver (21). The low level of ^{18}F radioactivity in blood is consistent with the hydrophilic metabolites (other than $[^{18}\text{F}]$ fluoride) being sulfoxy dicarboxylic acids which are cleared from the bloodstream efficiently by the kidneys (21).

Metabolic Trapping Ideology

Regional myocardial time-activity curves by PET following administration of a metabolically trapped LCFA tracer such as FTTHA may be suitable for quantitative modeling. The technique would require the building of a tracer kinetic model which describes the biochemistry and physiology involved and provides meaningful and statistically stable parameter estimates.

LCFAs are transported to myocytes through the mediation of various binding proteins in the endothelial, interstitial, and intracellular spaces (32). A transendothelial transporter of LCFAs has also been proposed (32). LCFAs

are metabolically sequestered within the cytosol of myocytes by the process of activation. The rate of activation of LCFA is dependent on the concentration of substrates (LCFA, CoASH, ATP) and products (long-chain acyl-CoA (LCACA), AMP, ADP), and the activity of long-chain acyl-CoA synthetase (3). Normally, the activation rate is regulated by changes in these factors, maintaining a flux which is coupled with the mitochondrial β -oxidation rate. However, in certain conditions such as ischemia, the activation rate and the β -oxidation rate may not be strongly coupled (3). The subsequent metabolic fate of LCACAs can be grouped into three main pathways: (1) transfer to carnitine by CPT I for eventual β -oxidation within the mitochondrion; (2) transfer to glycerol 3-phosphate, diacylglycerol, or lysophosphatidate toward the synthesis of various complex lipids (esterification); and (3) hydrolysis by long chain acyl-CoA hydrolase to regenerate free-fatty acid. The low myocardial content and rapid turnover of cytosolic LCACA would render the size of the LCACA pool and rates of LCACA hydrolysis inestimable using external measurements with an LCFA tracer (42).

In principle, however, the utilization rate of LCACAs for oxidation or esterification could be indicated by the accumulation of metabolic products beyond the activation step. If the radiotracer were incorporated into complex lipids, its regeneration by lipolysis and subsequent clearance from the myocardium could presumably be differentiated from the more rapid backdiffusion of nonmetabolized radiotracer in myocardial time-activity curves. However, β -oxidation of the radiotracer must give rise to metabolites that are retained within the myocardium for a sufficient time to allow a similar differentiation between their clearance and backdiffusion of nonmetabolized tracer. If so, then the accumulation of radioactivity in the myocardium would indicate the net utilization rate of LCFA, which would be the sum of the rates of esterification and oxidation. If, furthermore, the oxidative metabolites were completely retained in myocardium, and the myocardial kinetics could be observed for a long enough time (1–2 hr), then at least some fraction of the total accumulation rate due to esterification could be kinetically discriminated.

A better solution to the esterification-oxidation dilemma would be to design a radiotracer which specifically traces the β -oxidation pathway. In this case, the ideal PET LCFA tracer should not only have a terminal catabolite which is formed after commitment to β -oxidation and which has a very slow clearance, but should also yield a cytosolic acyl-CoA which is a very poor substrate for synthesis of complex lipids (10). It may not be possible to satisfy these criteria given the nature of the enzymes involved. The ability of the myocardial kinetics of such a radiotracer to specifically reflect LCFA β -oxidation rate rather than LCFA activation rate, especially in conditions when these two rates are not coupled, would depend on the hydrolytic rate of its acyl-CoA.

A PET technique based upon the myocardial time-activity curves of a metabolically trapped LCFA tracer would have several advantages. The relatively constant tissue concentrations of radioactivity following the uptake of a metabolically trapped LCFA radiotracer would allow accurate quantitation with PET. Data acquisition protocols would be less critical than with β -oxidizable LCFA radiotracers. The accumulation rate of radioactivity in the myocardium would directly reflect the utilization rate of LCFA. The effects of myocardial perfusion on the clearance kinetics would be separated from those due to metabolism because the metabolic products are retained. Finally, the simplified kinetics of a metabolically trapped LCFA may allow quantitation of transport and utilization rate through the application of appropriate tracer kinetic models.

CONCLUSIONS

From a practical standpoint, its high myocardial uptake, long myocardial retention, and rapid clearance from the bloodstream would make FTHA a useful myocardial imaging agent for PET. More importantly, the myocardial kinetics of ^{18}F radioactivity with administration of FTHA may sensitively indicate the β -oxidation rate of LCFA. This may provide important metabolic information in addition to the total oxidative metabolic rate indicated by [^{11}C] acetate. Further studies are encouraged to understand the radiopharmacology of FTHA in a variety of conditions and test its applicability to a quantitative PET technique for noninvasive measurement of LCFA utilization.

ACKNOWLEDGMENTS

The authors wish to thank Mr. W. Wutz for his excellent technical assistance. We are also grateful for the helpful suggestions and comments of Dr. S. John Gatley.

REFERENCES

1. Brown M, Marshall DR, Sobel BE, Bergmann SR. Delineation of myocardial oxygen utilization with carbon-11-labeled acetate. *Circulation* 1987;76:687–696.
2. Buxton DB, Schwaiger M, Nguyen A, Phelps ME, Schelbert HR. Radiolabeled acetate as a tracer of myocardial tricarboxylic acid cycle flux. *Circ Res* 1988;63:628–634.
3. Wenger JI, Neely JR. Regulation of uptake and metabolism of fatty acids by muscle. In: Dietschy JM, Gotto AM Jr, Ontka JA, eds. *Disturbances in lipid and lipoprotein metabolism*. Bethesda: American Physiological Society; 1978:269–284.
4. Schelbert HR, Schwaiger M. PET studies of the heart. In: Phelps M, Mazziotta JC, Schelbert HR, eds. *Positron emission tomography and autoradiography. Principles and applications for the brain and heart*. New York: Raven Press; 1986:581–661.
5. Fox KAA, Abendschein DR, Ambos HD, Sobel BE, Bergmann SR. Effects of metabolized and nonmetabolized fatty acid from canine myocardium: implications for quantifying myocardial metabolism tomographically. *Circ Res* 1985;57:232–243.
6. Rosamond TL, Abendschein DR, Sobel BE, Bergmann SR, Fox KAA. Metabolic fate of radiolabeled palmitate in ischemic canine myocardium: implications for positron emission tomography. *J Nucl Med* 1987;28:1322–1329.

7. Wyns W, Schwaiger M, Huang SC, Buxton DB, Hansen H, Selin C, Keen R, Phelps ME, Schelbert HR. Effects of inhibition of fatty acid oxidation on myocardial kinetics of ¹⁴C-labeled palmitate. *Circ Res* 1989;65:1787-1797.
8. Knust EJ, Kupfernagel C, Stöcklin G. Long-chain F-18 fatty acids for the study of regional metabolism in heart and liver; odd-even effects of metabolism in mice. *J Nucl Med* 1979;20:1170-1175.
9. Kloster G, Stöcklin G, Smith EF, Schrör K. ω -Halofatty acids: a probe for mitochondrial membrane integrity. In vitro investigations in normal and ischaemic myocardium. *Eur J Nucl Med* 1984;9:305-311.
10. Gatley SJ, DeGrado TR, Kornguth ML, Holden JE. The development of new, innovative PET radiopharmaceuticals for measuring the rates of physiological and biochemical processes. *Acta Radiologica* 1991:in press.
11. Berridge MS, Tewson TJ, Welch MJ. Synthesis of ¹⁸F-labeled 6- and 7-fluoropalmitic acids. *Int J Appl Radiat Isot* 1983;34:727-730.
12. Elmaleh DR, Livni E, Levy S, Varnum D, Strauss HW, Brownell GL. Comparison of ¹¹C and ¹⁴C-labeled fatty acids and their β -methyl analogs. *Int J Nucl Med Biol* 1983;10:181-187.
13. Abendschein DR, Fox KAA, Ambos HD, Sobel BE, Bergmann SR. Metabolism of beta-methyl[1-¹⁴C]heptadecanoic acid in canine myocardium. *Nucl Med Biol* 1987;14:579-585.
14. Fink GD, Montgomery JA, David F, Garneau M, Livni E, Elmaleh D, Strauss HW, Brunengraber H. Metabolism of β -methyl-heptadecanoic acid in the perfused rat heart and liver. *J Nucl Med* 1990;31:1823-1830.
15. Nishimura S, Takahashi T, Ido T, Ishiwata K, Iwata R. Development of branched-chain [¹⁸F]fluorofatty acids for evaluating regional β -oxidation in the heart [Abstract]. *J Nucl Med* 1990;31:901.
16. Knapp FF, Srivastava PC, Callahan AP, Cunningham EB, Kabalka GW, Sastry KAR. Effect of tellurium position on the myocardial uptake of radioiodinated 18-iodotellura-17-octadecenoic acid analogues. *J Med Chem* 1984;27:57-63.
17. Okada RD, Knapp FF, Goodman MM, Elmaleh D, Strauss HW. Tellurium-labeled fatty acid analogs: relationship of heteroatom position to myocardial kinetics. *Eur J Nucl Med* 1985;11:156-161.
18. Lau SM, Brantley RK, Thorpe C. The reductive half-reaction in acyl-CoA dehydrogenase from pig kidney: studies with thiooctanoyl-CoA and oxoac-tanoyl-CoA analogues. *Biochemistry* 1988;27:5089-5095.
19. Lau SM, Brantley RK, Thorpe C. 4-Thia-trans-2-alkenoyl-CoA derivatives: properties and enzymatic reactions. *Biochemistry* 1989;28:8255-8262.
20. Skrede S, Narce M, Bergseth S, Bremer J. The effects of alkylthioacetic acids (3-thia fatty acids) on fatty acid metabolism in isolated hepatocytes. *Biochim Biophys Acta* 1989;1005:296-302.
21. Bergseth S, Bremer J. Alkylthioacetic acids (3-thia fatty acids) are metabolized and excreted as shortened dicarboxylic acids in vivo. *Biochim Biophys Acta* 1990;1044:237-242.
22. Hovik R, Osmundsen H, Berge R, Aarsland A, Bergseth S, Bremer J. Effects of thia-substituted fatty acids on mitochondrial and peroxisomal β -oxidation. Studies in vivo and in vitro. *Biochem J* 1990;270:167-173.
23. Heuckeroth RO, Glaser L, Gordon JI. Heteroatom-substituted fatty acid analogs as substrates for N-myristoyltransferase: an approach for studying both the enzymology and function of protein acylation. *Proc Natl Acad Sci USA* 1988;85:8795-8799.
24. Rahman MD, Ziering DL, Mannarelli SJ, Swartz KL, Huang DS, Pascal RA. Effects of sulfur-containing analogues of stearic acid on growth and fatty acid biosynthesis in the protozoan *Crithidia fasciculata*. *J Med Chem* 1988;31:1656-1659.
25. DeGrado TR, Stöcklin G. 14(R,S)-[F-18]Fluoro-6-thia-heptadecanoic acid (FTHA): a new in vivo probe for measurement of myocardial long chain fatty acid (LCFA) utilization [Abstract]. *J Nucl Med* 1991; 32:937.
26. DeGrado TR. Synthesis of 14(R,S)-[¹⁸F]fluoro-6-thia-heptadecanoic acid (FTHA). *J Lab Comp Radiopharm*;1991:in press.
27. Coenen HH, Klatte B, Knöchel A, Schüller M, Stöcklin G. Preparation of n.c.a. [17-¹⁸F]-fluoroheptadecanoic acid in high yields via aminopolyether supported, nucleophilic fluorination. *J Lab Compd Radiopharm* 1986;23:455-466.
28. DeGrado TR, Moka DC. Non- β -oxidizable ω -[¹⁸F]fluoro long chain fatty (LCFA) analogs show cytochrome P-450 mediated defluorination: Implications for the design of PET tracers of myocardial fatty acid utilization. *Nucl Med Biol* 1991:in press.
29. Cleland WW. Dithiothreitol, a new protective reagent for SH groups. *Biochemistry* 1964;3:480-482.
30. Rosenthal MS, Bosch AL, Nickles RJ, Gatley SJ. Synthesis and some characteristics of no-carrier-added [¹⁸F]fluorotrimethylsilane. *Int J Appl Radiat Isot* 1985;36:318-319.
31. Machulla HJ, Stöcklin G, Kupfernagel C, Freundlieb C, Höck A, Vyska K, Feinendegen LE. Comparative evaluation of fatty acids labeled with C-11, C1-34m, Br-77, and I-123 for metabolic studies of the myocardium: concise communication. *J Nucl Med* 1978;19:298-302.
32. Bassingthwaite JB, Noodleman L, van der Vusse G, Glatz JFC. Modeling of palmitate transport in the heart. *Mol Cell Biochem* 1989;88:51-58.
33. DeGrado TR, Holden JE, Ng CK, Raffel DM, Gatley SJ. Quantitative analysis of myocardial kinetics of 15-p-[iodine-125]iodophenylpentadecanoic acid. *J Nucl Med* 1989;30:1211-1218.
34. DeGrado TR. PhD Thesis. University of Wisconsin-Madison 1988.
35. Paulson DJ, Noonan JJ, Ward KM, Sherratt HSA, Shug AL. Effects of POCA on metabolism and function in the ischemic rat heart. *Basic Res Cardiol* 1986;81:180-187.
36. Declercq PE, Venincasa MD, Mills SE, Foster DW, McGarry JD. Interaction of malonyl-CoA and 2-tetradecylglycidyl-CoA with mitochondrial carnitine palmitoyltransferase I. *J Biol Chem* 1985;260:12516-12522.
37. Wilms J, Lub J, Wever R. Reactions of mercaptans with cytochrome c oxidase and cytochrome c. *Biochim Biophys Acta* 1980;589:324-335.
38. Olson RE, Hoeschen RJ. Utilization of endogenous lipid by the isolated perfused rat heart. *Biochem J* 1967;103:796-801.
39. Crass MF, McCaskill ES, Shipp JC, Murthy VK. Metabolism of endogenous lipids in cardiac muscle: effect of pressure development. *Am J Physiol* 1971;220:428-435.
40. Bonte FJ, Parkey RW, Graham KD, Moore JG. Distributions of several agents useful in imaging myocardial infarcts. *J Nucl Med* 1975;16:132-135.
41. Sykes TR, Quastel JH, Adam MJ, Ruth TJ, And Noujaim, AA. The disposition and metabolism of [¹⁸F]-fluoroacetate in mice. *Biochem Arch* 1987;3:317-323.
42. Idell-Wenger JA, Grotzjohann LW, Neely JR. Coenzyme A and carnitine distribution in normal and ischemic hearts. *J Biol Chem* 1978;253:4310-4318.